Assimilation of Earth Observation Data for Crop Yield Estimation in Smallholder Agricultural Systems

Biniam Sisheber, Michael Marshall, Daniel Mengistu, and Andrew Nelson

***Abstract*—Crop yield estimates are an important data output of agricultural monitoring systems. In sub-Saharan Africa, large input requirements of crop growth models, fragmented agricultural systems, and small field sizes are substantial challenges to accurately estimate crop yield. Multisensor data fusion can be a valuable source of high spatial and temporal resolution data to meet the requirements of crop growth models in Africa. In this study, we estimated crop yield in smallholder agricultural systems of Ethiopia by assimilating Landsat and MODIS fused data in the simple algorithm for crop yield estimation (SAFY) model. Enhanced spatial and temporal adaptive reflectance fusion model (ESTARFM) adapted for fragmented agricultural landscapes was used for data fusion. We assimilated LAI and phenology information derived from Landsat–MODIS fusion, MODIS and field data for comparison. The model was validated with in situ LAI and yield measured in rice and maize fields during the 2019 growing season. Data fusion minimized the yield estimation error (rRMSE = 16% for maize and rRMSE = 23% in rice) more than MODIS (rRMSE = 20% for maize and rRMSE = 35% in rice) because of its higher LAI and phenology estimation accuracy. Data fusion improved the calibration accuracy of the field and crop-specific model parameters and better captured the spatial variability of yield, which is vital for crop production monitoring and food security in smallholder agricultural systems in Africa. Considering the promising results, further investigation into the transferability of the approach to other smallholder agricultural landscapes and hybridization with machine learning is needed for large-area applications.**

***Index Terms*—Agricultural production, crop modeling, data fusion, phenology, remote sensing.**

Manuscript received 30 August 2023; revised 24 October 2023; accepted 28 October 2023. Date of publication 1 November 2023; date of current version 29 November 2023. This work was supported in part by the Dutch Organization for Internationalization in Education (Nuffic), in part by the Faculty of Geo-Information Science and Earth Observation (ITC), University of Twente, and in part by the Ministry of Science and Higher Education of Ethiopia (MoSHE) under the Ethiopia Education Network to Support Agricultural Transformation (EENSAT) project under Grant CF13198,2016. *(Corresponding author: Biniam Sisheber.)*

Biniam Sisheber is with the Department of Natural Resources, Faculty of Geo-information Science and Earth Observation (ITC), University of Twente, 7522 NH Enschede, The Netherlands, and also with Geospatial Data and Technology Center (GDTC) and Department of Geography and Environmental Studies, Bahir Dar University, Bahir Dar 6000, Ethiopia (e-mail: biniamsisheber@gmail.com).

Michael Marshall and Andrew Nelson are with the Department of Natural Resources, Faculty of Geo-information Science and Earth Observation (ITC), University of Twente, 7522 NH Enschede, The Netherlands (e-mail: m.t.marshall@utwente.nl; a.nelson@utwente.nl).

Daniel Mengistu is with the Geospatial Data and Technology Center (GDTC) and Department of Geography and Environmental Studies, Bahir Dar University, Bahir Dar 6000, Ethiopia (e-mail: dan952003@yahoo.com).

This article has supplementary downloadable material available at https://doi.org/10.1109/JSTARS.2023.3329237, provided by the authors.

Digital Object Identifier 10.1109/JSTARS.2023.3329237

I. Introduction

CROP production is the dominant means of livelihood and food security in smallholder farming systems [1]. Climate change, recurrent drought, land degradation, and soil infertility contribute to high interannual variability in crop production and the source of food insecurity for a growing population [2]. Field-level crop yield estimation informs the status of crop production and food insecurity in smallholder farming communities [3]. In sub-Saharan Africa, traditional crop yield estimation methods by national governments through fieldwork are laborious, time-consuming, and inaccurate in capturing fragmented ($\leq$1ha) arable lands [4]. Earth observation (EO) satellite data can be used for spatially explicit crop yield estimation in smallholder agricultural systems.

EO data is increasingly used for yield estimation with the emergence of open-access high spatiotemporal multispectral data [5]. Higher spatial resolution ($\leq$30 m) and frequent (daily to 8-day) EO data are necessary to capture the spatial heterogeneity of croplands in fragmented and persistently cloudy environments [6]. The Moderate Resolution Imaging Spectroradiometer (MODIS) data have been widely used for its daily temporal coverage in relatively homogeneous agricultural regions [7]. However, with a spatial resolution of 250–500 m, it is difficult to discern individual fields in most African agricultural landscapes [4]. High spatial resolution sensors such as Landsat (30 m) and Sentinel-2 (10–60 m) are inadequate for monitoring crop growth and development because of persistent cloud cover during the main crop-growing seasons [6]. Multisensor data fusion is one option to obtain frequent cloud-free observations at high spatial resolution in such environments.

Spatiotemporal data fusion provides enhanced information for yield estimation by integrating low spatial/high temporal with high spatial/low temporal resolution data [4], [8]. For instance, Gao et al. [8] fused Landsat–MODIS and Landsat–Sentinel-2-MODIS to capture the field scale crop yield variability in the United States Corn Belt. Combined use of LAI derived from fused data and Landsat [9], harmonized Landsat-8 and Sentinel-2 [10] improved yield estimation in Canada. These studies indicated that data fusion offers the high spatial and temporal resolution of EO data to improve crop yield estimation. However, in smallholder farming systems, addressing the limitation of data fusion algorithms is important to detect the spatial and temporal crop growth changes when frequent Landsat observations are unavailable [8]. The enhanced spatial and temporal adaptive reflectance fusion model (ESTARFM)

[11] has been modified with knowledge-based input and similar pixel selection criteria aimed to capture phenology change due to infrequent Landsat input acquisitions [12]. The modified ESTARFM uses crop calendar information to distribute input images and a land cover map to select similar pixels from homogenous land cover classes. The model has been evaluated in fragmented agricultural landscapes with ground-measured LAI, sowing and harvest date information, where it reduced the root mean square error (RMSE) of emergence date from 17 days with MODIS to 7 days [12]. Integrating data fusion in crop growth model through data assimilation can be an opportunity to estimate crop yield in smallholder agricultural systems.

EO data have been assimilated into various process-based crop growth models for large-area crop yield estimations [10], [13], [14], [15], [16]. Data assimilation remains challenging because the models require field scale inputs and frequent high spatial resolution EOs, often freely unavailable in smallholder agricultural systems [17]. Data assimilation in semiempirical models, designed based on Monteith [18] light use efficiency (LUE), have been widely used due to their relatively low data demands [19], [20]. In this regard, the simple algorithm for yield estimates (SAFY) [21] overcomes the limitations arising from complicated parameterization and translates EO-derived biochemical properties of crops into total biomass and yield [22]. Studies showed that coupling SAFY with EO improved regional and field-level yield estimation in various agroecosystems [10], [16], [22], [23]. Nevertheless, there is a lack of reliable yield estimation in most African agricultural landscapes because of the difficulty of obtaining the frequent high spatial resolution data requirements of crop models [4]. The few studies estimating crop yield based on empirical relationships between EO data and ground measurements usually unable to account for crops' biophysical processes and are unsuitable for applying over dynamic geographical regions and growing seasons [1], [2], [3]. These studies also indicated the importance of obtaining high spatial resolution EO data to capture the small field size in Africa. Coupling simple crop models with Landsat–MODIS fusion can be a feasible solution to obtain the frequent high spatial resolution input requirements of the crop model to improve field-level yield estimation, which needs investigation in smallholder agricultural systems in Africa.

This study aims to estimate crop yield by assimilating data fusion retrieved LAI and phenology to improve spatial variability of yield estimation in a smallholders agricultural systems in Ethiopia. Optimizing model parameters contributing to capture the spatial variability of crop yield is important to improve yield estimation in smallholder agricultural systems. Thus, we evaluated the sensitivity of calibrating the SAFY crop model with Landsat and MODIS data fusion and MODIS without fusion. We first determined phenological parameters and LAI from fused data and MODIS to optimize the SAFY crop model. Second, we present a sensitivity analysis of model parameters to prioritize the parameters during calibration, and validated SAFY simulation outputs (LAI, and yield) to examine the performance of the model. Finally, we analyzed the factors affecting the spatial variability of estimated yield to highlight parameters requiring attention when estimating yield in smallholder agricultural systems. An improved crop yield model based on data fusion in the smallholder agricultural systems in this study is vital to assist crop production monitoring and food security analysis.

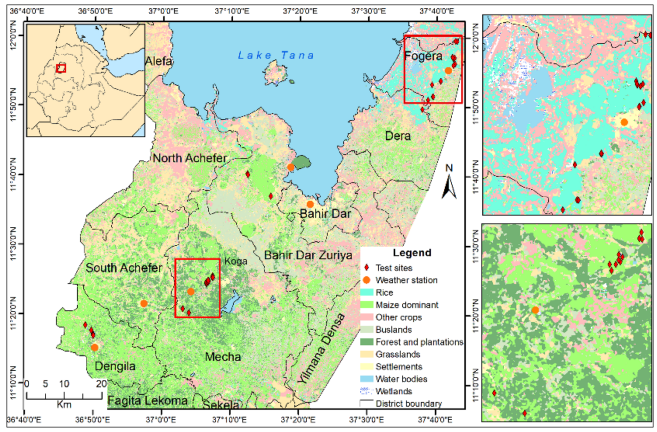

Fig. 1. Map of the study area showing the distribution of maize (south of Lake Tana) and rice (Fogera) samples and Land cover map of the study area for the 2019 growing season [12].

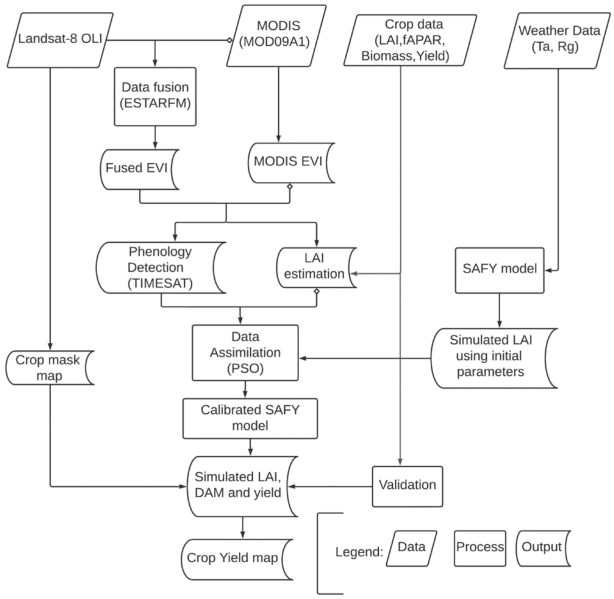

Fig. 2. Technical workflow.

II. Materials

A. Study Area

The study was conducted in major crop-growing districts in the Lake Tana sub-basin of the upper Blue Nile basin in Ethiopia (see Fig. 1). The elevation ranges from 1700 to 3500 meters above sea level, the mean temperature ranges between 13 °C to 22 °C, and the mean annual precipitation ranges between 970 and 1900 mm. The main rainy season (locally called "Kiremt") occurs between June and September. It supports the main ("Meher") crop production. The northward movement of

the inter-tropical convergent zone (ITCZ) drives the main rainy season ("Kiremt"). A short and highly variable rainfall period also occurs between March and May (" Belg"), while October to January ("Bega") is the dry season that also influences Meher crop production. Crop production is mainly rainfed and stratified by climatology and topography. The highlands are fragmented, contain small fields (<1 ha), and receive the largest amount of rainfall [24]. The central districts (Bahir Dar Zuria, Dera, and Mecha) have plains and undulating topography supporting maize cultivation. Rice is cultivated in the lowland floodplain east of Lake Tana (Fogera).

B. Description of the Crop Growth Model

We used SAFY for biomass and yield estimation for its low input requirements, but comparable performance to fully process-based crop models and data-driven methods [16], [19], [23], [25]. Unlike most general crop models such as World Food Studies (WOFOST), SAFY does not require soil-water and crop parameters [13], which are often unavailable or highly uncertain in many agricultural landscapes in Africa. The few data and parameter requirement of SAFY is vital to minimize model simulation error due to data uncertainty in the study area.

SAFY has been designed to estimate daily LAI, dry aboveground biomass (DAM) and grain yield from the date of emergence to the end of senescence based on the Monteith [18] LUE model and Maas [26] leaf partitioning theory. DAM is driven by absorbed photosynthetically active radiation (APAR), and effective LUE (ELUE) is constrained by the daily mean temperature (Ta) and defined as (1). APAR, the fraction of incoming shortwave radiation captured by green plants pigments for photosynthesis, is determined as the product of incoming shortwave radiation (Rg), climate efficiency coefficient, and fAPAR [see (2)]. fAPAR is estimated using Beer's law [see (3)], where K defines the light interception coefficient of crops. The temperature stress factor, which represents the effect of temperature in the conversion of intercepted solar radiation into plant biomass is determined as polynomial degree (β) of optimal mean daily temperature (T_{opt}) and two extreme temperatures ($T_{\max}$, $T_{\min}$), beyond which crop stop growth [see (4)].

$$\text{DAM} = \text{ELUE} * \text{APAR} * \text{Ft}\,(Ta) \tag{1}$$

$$\text{APAR} = \text{Rg} * \varepsilon\text{C} * \text{fAPAR} \tag{2}$$

$$\text{fAPAR} = 1 - \exp\,(-k * \text{LAI}) \tag{3}$$

$$\text{FT}\;(Ta) = 1 - \left\{\frac{T_{\text{opt}} - \text{Ta}}{T_{\text{opt}} - T_{\min}}\right\}\beta,$$

$$\text{if } T_{\min} \left\langle Ta \left\langle T_{\text{opt}}; = 1 - \left\{\frac{\text{T}_{\text{opt}} - \text{Ta}}{\text{T}_{\text{opt}} - \text{T}_{\max}}\right\}\beta \ldots, \text{ if } T_{\max} \right\rangle Ta \right\rangle$$

$$\times\, T_{\text{opt}};\; 0 \ldots \text{ if } Ta\,\langle T_{\min} \text{or}\; Ta\rangle\, T_{\max}. \tag{4}$$

LAI simulation is divided into vegetative and senescence stages. During the vegetative stage, LAI increases [ΔLAI+: (6)] as the fraction of daily ΔDAM partitioned to leaf growth through the partitioning function [Pl: (5)] modulated by the specific leaf area of crops (SLA). Pla and Plb are the partitioning parameters that determine the magnitude and shape of LAI and the daily sum of temperature (SMT) [21]. LAI tends to decrease (ΔLAI-) (7) when SMT reaches a certain threshold (S_{TT}: Sum of temperature for senescence) controlled by the rate of senescence (Rs). Fig. 1 shows the yield estimation workflow of the study.

$$\text{Pl}\left(\sum Ta\right) = 1 - \text{Pla} \times e^{\text{plb}\times\text{STM}} \tag{5}$$

$$\Delta\text{LAI}+ = \Delta\text{DAM} \times \text{Pl}\left(\sum Ta\right) \times \text{SLA},\; \text{Pl} > 0 \tag{6}$$

$$\Delta\text{LAI}- = \text{LAI} \times (\text{SMT} - S_{\text{TT}})/\text{Rs}),\; \text{SMT} > S_{\text{TT}}. \tag{7}$$

C. Field Data

We collected LAI, fAPAR, biomass, and yield from maize and rice fields during the 2019 growing season. We also obtained crop growth information (sowing and harvest dates, crop height, and crop density) to support our analysis (see supplementary material, Table SI). The average maize sowing date was 20 June to 10 July for rice and harvested from 27 November to 6 December; maize was sowed from 5–15 June and harvested between 18 November and 23 December during the 2019 growing season.

1) *LAI and fAPAR acquisition:* We collected LAI and fAPAR from 33 farm fields randomly stratified by crop type (maize and rice) (see Fig. 1). A total of 142 LAI and 84 fAPAR samples were measured from July to December 2019 at the green-up stage, heading, reproductive, and maturity stages of maize and rice crops (see supplementary material, Table SI). We used a Decagon AccuPAR ceptometer to obtain LAI and fAPAR measurements. Standard procedures for ceptometer deployment and calibration were followed as outlined in the device manual and as recommended by Marshall and Thenkabail [27]. LAI and fAPAR were sampled over 60 m × 60 m elementary sampling units (ESUs) to account for geo-location error between the field measurements and Landsat ground sampling distance of 30 m. Larger 90 m × 90 m ESUs would have been ideal for the study, but were not possible because of the small sizes of the fields. Within each ESU, ten LAI readings (averaged from multiple positions within the canopy) were recorded in 1 m × 1 m quadrats. The results were averaged to one LAI reading per ESU.
2) *Biomass and Yield acquisition:* We harvested the grain and straw from 16 rice farm fields in two to three subplots within a 0.25 m × 0.25 m (0.0625 m^2) area. For maize, we used the yield component method to harvest ears from 17 farm fields and counted the number of ears per 5-m^2 area, kernel rows per ear, kernels per row, and kernel weight after oven drying. The rice straw, grain, and maize ear samples were dried at a temperature of 80 °C for 72 h, and the total yield was calculated in grams per square meter. We acquired an additional 14 rice yield samples from farmers' reporting.
3) *Metrological data:* Daily solar radiation and mean daily temperature are the two climate-forcing variables in

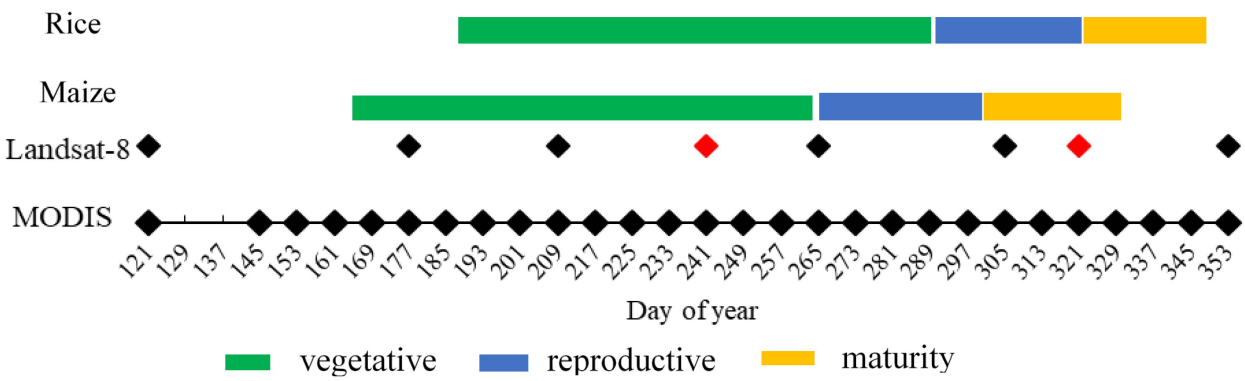

Fig. 3. Landsat and MODIS acquisition dates. The back diamond shapes indicate inputs used for prediction, while the red was used for validation.

SAFY. The incoming short-wave radiation was obtained from NASA's Modern-Era Retrospective Analysis for Research and Applications (MERRA-2) (https://disc.sci.gsfc.nasa.gov), which is a reanalysis product with a spatial resolution of 0.5° latitude by 0.67° longitude. We acquired temperature records from the National Metrological Agency of Ethiopia (NMA) and a ground weather station installed in July 2019 within a 5–25 km radius of maize sample fields. The station collects solar radiation (W/m^2) and PAR (W/m^2) measured using light quantum sensor and temperature (°C) with 15-min timestamp. A comparison of the MERRA-2 radiation and the ground measurements showed an error of 2.9 MJ/m^2/day, which can be considered reasonably accurate in the study area.

4) *Crop mask*: Field-level crop yield simulation requires a crop mask. In this study, we used a land cover map (see Fig. 1) classified in 2019 from Landsat-8 [12] using a support-vector machine model to filter rice and maize fields from other land cover classes. The land cover map discriminated maize and rice from other land cover units with an overall accuracy of 82.9%, a kappa coefficient of 0.80, a user's accuracy of 79%, and a producer's accuracy of 78%. We used crop calendar information and EVI empirical thresholds similar to Bolton and Friedl [28] to minimize misclassification and exclude other crop types from the analysis. Crop pixels with a green up in late June and early July (EVI $>$ 0.25) that reached a peak value before the end of September (EVI$>$ 0.6) were classified as maize after comparison against the ground sowing date information. Rice grows uniformly only in the Fogera floodplain area and rice pixels outside the area were excluded. We masked maize (2120 km^2) and rice (258 km^2) fields for the final pixel-level yield simulation.

D. Satellite Image Data

Level-2 terrain corrected Landsat-8 data were acquired from the United States Geological Survey (USGS) Earth Explorer (https://earthexplorer.usgs.gov/) for path/row: 170/52 in 2019. To get reliable surface reflectance data, the USGS applied atmospheric correction using the Landsat-8 Surface Reflectance Code (LaSRC), improved aerosol determination [29]. We obtained five low cloud cover Landsat images with $\leq$30% for data fusion input and two for validation from May to December to cover the rice and maize crop-growing season after assessment of the scene level cloud cover within the boundary of the study area. Fig. 3 shows the distribution of Landsat inputs.

The MODIS surface reflectance data (MOD09A1: V006.1) was acquired from NASA's LP DAAC website (https://lpdaac.usgs.gov/) for image tile: 21/7 horizontal/ vertical over the study period. The product consists of atmospheric, and aerosol corrected surface reflectance spectral bands at 500-m spatial resolution and composited over 8-day intervals. We reampled the MODIS data to WGS84 UTM zone 37 and 30 m with nearest neighbor to match the Landsat projection and resolution.

We used six of the Landsat and MODIS bands (blue, green, red, NIR, SWIR1, and SWIR2) for data fusion since more bands improve feature separability during fusion. Landsat and MODIS were used for data fusion for consistency of the sensors' spectral characteristics [29]. The Landsat pixel quality and MODIS state flag bands were used to flag low-quality pixels.

III. Methods

A. Landsat–MODIS Fusion

Higher spatial resolution EO data are crucial to determine the phenological and agronomic parameters for field-level yield estimation. We used ESTARFM [11], modified for fragmented agricultural landscapes [12], to fuse Landsat-8 OLI and MODIS (MOD09A1) in the 2019 growing season to obtain the frequent high-resolution data requirement. We selected pairs of Landsat and MODIS images at two base dates (t_0) before (t_1) and after (t_2) the prediction dates (t_p) and MODIS images at every prediction date for Landsat–MODIS data fusion. In the modified ESTARFM, we distributed the Landsat inputs at the vegetative, reproductive, and maturity stages based on the maize and rice crop calendar (see Fig. 3) to minimize the effect of reflectance change between t_0 and t_p during the model prediction. When frequent cloud-free Landsat inputs were available, we selected the Landsat and MODIS inputs with similar acquisition dates. When available cloud-free Landsat inputs were at different phenological stages of crops, we used the MODIS composite best

correlated with MODIS input at t_p and with Landsat at the base dates (MODIS t_0–t_p correlation) to compensate for phenology change. Then, similar pixels were flagged based on the intersection of Landsat reflectance at t_1 and t_2 in a moving window (w) size of 50×50 Landsat pixels and homogeneous land cover class (c). We used the land cover map (see Fig. 1) as input to select similar pixels from the same land cover class. Due to the small field size and variation of management practice, adequate similar pixels (>20 pixels) for prediction were obtained when $c = 6$ for vegetative growth stage prediction and $c = 4$ during the other periods. Details of the modified input and similar pixel selection workflow are provided in the supplementary material. Finally, the spatial weighting function (w_i) and conversion coefficient (v_i) were calculated based on the original ESTARFM.

The enhanced vegetation index (EVI) was calculated [30] from the Landsat–MODIS fused and MODIS to determine crop phenology and estimate LAI for its resistant to saturation than NDVI common in high-canopy crops [31]. Validation of the fused data with original Landsat input showed acceptable accuracy (see Fig. S1 supplementary material and [12]).

B. Crop Phenology Detection

Accurate phenology estimation is crucial for SAFY to capture field-level yield variability [22]. The key phenological dates and stages required are the start of season (SOS), representing the emergence date; the peak of season (POS), used to determine the day of senescence (DOS) and the end of season (EOS), which is the termination of the model simulation. We used the Savtizky–Golay (S-G) smoothing and seasonal amplitude (dynamic threshold) method [32] to determine the phenological parameters with the TIMESAT software package (see suplementary matterial). The phenological parameters were forced as input values in SAFY model to improve spatial variability of yield estimates.

C. LAI and fAPAR Estimation

Pixel level LAI was estimated from Landsat–MODIS fusion and MODIS-derived EVI time series to calibrate SAFY parameters. EVI smoothed with an S–G filter was used for LAI estimation to minimize distortion from cloud, data fusion uncertainty, and mixed pixel problems. We fitted an empirical relationship between in situ LAI and smoothed EVI to estimate LAI time series. The exponential function best fitted in both maize and rice (see supplementary material, Fig. S2), and the equations were applied to the 8-day Landsat–MODIS fused (hereafter F_{LAI}) and MODIS (hereafter M_{LAI}) in rice and maize pixels from SOS to EOS dates. We estimated fAPAR based on the Beer–Lambert law [see (3)] to determine the light interception efficiency of crops (k) and evaluate the pixel level calibration of the ELUE, as fAPAR is an effective estimator of the ELUE [17], [33]. The coefficient of determination (R^2), the root mean square error (RMSE), and the relative root mean square error (rRMSE) were used to assess the fitness and robustness of LAI and fAPAR estimations.

D. Data Assimilation in the SAFY Model

We used the calibration approach to assimilate F_{LAI} and M_{LAI} into SAFY because it can minimize the error of EO data [34]. In previous studies, SAFY has been modified to include soil water content parameters [35]. However, uncertainty in soil water content and management practice data can lead to systematic error [36] and increased model complexity [37]. Instead, the pixel level LAI and ELUE account for agro-environmental stress factors [19], [22], [23]. Therefore, we maintained the simplicity of the original model with 15 parameters by introducing a few modifications to detect the spatial variation of crop yield in the smallholder agricultural landscapes. First, we used the pixel-level phenology information (D_0, S_{TT}, and EOS) determined from phenology detection method as initial input variables to reduce the systematic error that could occur due to calibration of several sensitive parameters [22] and to capture field level yield variation. Second, the remaining sensitive parameters of SAFY were calibrated using continuous (8-days) LAI estimated from Landsat–MODIS fused. Finally, we adjusted the values of the fixed parameters and the range of calibrated parameters through field measurements because a narrow fit of parameter ranges increases the calibration accuracy. The ranges of calibrated parameters of the SAFY model used in this study are presented in Table I. We also run the model using LAI and phenology information derived from MODIS and field data, for comparison.

1) *Fixed and input parameter values:* The prior parameters are conservative and fixed throughout the growing season, which was determined from literature and in situ observations. DAM_0 was fixed according to previous studies after comparing it to the local area with emergence date LAI, and SLA. The three temperature values (T_{opt}, T_{max}, and T_{min}) for canopy development were obtained for maize and rice from studies conducted in similar crop growing environments. We calculated the climate efficiency as the ratio of daily PAR and shortwave radiation measured using light quantum sensors installed in our weather station. The light extinction coefficient (k) was calculated from measured peak season LAI and fAPAR using (3). Harvest index (HI), the ratio of grain yield to the total amount of DAM generated, was calculated for rice from ground data and based on [40] for maize.

Pixel-level phenological information determined from the phenology detection method was used as input variables. The periods between SOS and EOS delimit the model simulation range. The SOS replaced D_0, which determined the time for starting LAI development and biomass accumulation. The S_{TT}, which constrains the value of LAI decrease during the senescence phase, was determined from aggregates of the mean daily temperature between D_0 and DOS.

2) *Calibration of parameters:* We calibrated four sensitive parameters of SAFY (Pla, Plb, Rs, and ELUE) [21], [37] using FLAI, MLAI, and field-measured LAI. LAI time series were assimilated from green up to reproductive stages (DOY 201 to DOY 297 for maize and DOY 225 to DOY 321 for rice). We used the particle swarm optimization (PSO) algorithm to run at the pixel level for its

TABLE I
INITIAL AND CALIBRATED VALUES OF SAFY MODEL PARAMETERS

Parameters		Rice	Maize	Source
	Unit	Range or value	Range or value	
Input variables				
Daily incoming global variation (Rg)	MJ m^{-2} d^{-1}	-	-	METRA2 and station
Daily mean air temperature (Ta)	°C	-	-	Weather stations
Fixed parameters				
Initial LAI	m^2/m^{-2}	0.02	0.1	LAI estimated
Initial dry aboveground mass (DAM_0)	kg ha^{-1}	2.0	4.0	[37]/[19]
Climatic efficiency (εC)	-	0.5	0.5	In situ measurement
Light-interception coefficient (k)		0.55	0.5	In situ measurement
Temperature for crop growth (T_{min}, T_{opt}, Tmax)	°C	10, 31, 42	10,30,45	[38, 39]
Polynomial degree (β)	-	2	2	[19]
Specific leaf area (SLA)	m^2 g^{-1}	0.019	0.024	[40]/[19]
Harvest index (HI)	-	0.25	0.5	In situ measurement/ [39]
Input parameter values				
Emergence date (D_0)	DOY	[185,220]	[170,190]	Phenology detection
Date of senescence (DOS)	DOY			Phenology detection
Sum of temperature for senescence (S_{TT})	°C	[1839,2226]	[1365,1920]	Ta from D_0 to DOS
End of simulation (EOS)	DOY			Phenology detection
Calibrated parameters				
Partition-to-leaf function: parm a (Pla)	-	[0.1,0.5]	[0.1,0.5]	Calibrated
Partition-to-leaf function: parm b (Plb)	-	[0.0007,0.0059]	[0.0007,0.002]	Calibrated
Rate of senescence (Rs)	°C d^{-1}	[4000, 15000]	[3000, 10000]	Calibrated
Effective LUE (ELUE)	g MJ^{-1}	[1.2, 4]	[1.5, 4]	Calibrated

simplicity, precision, and computational efficiency [16]. PSO assumes a group of m particles ($m = 30$ in this study based on the previous literature) with certain speeds without quality and size in n d-dimensional space. The particles modify their position and velocity based on the best point in the current generation ("personal best") and the best point of all particles in the swarm ("global best"). We applied a cost function (8) minimizing the RMSE of simulated SAFY LAI and EO estimated LAI to optimize SAFY.

The optimization involves calibrating crop-specific parameters (Pla, Plb, and R_S) in the first stage and the field-specific ELUE in the second stage. The vegetative stage parameters (Pla and Plb) describing the allocation of leaves to biomass during growth and the Rs, which are crop-specific parameters [21], were calibrated separately for rice and maize. We used the cross relationship of Pla and Plb based on (5) and the relationship between S_{TT} and SMT between D_0 to EOS for R_S to adjust the initial range of the parameters. ELUE, which represents the crop's ability to convert intercepted radiation to biomass and accounts for local stress factors [19], was calibrated for sample fields and pixel-by-pixel with LAI estimated from data fusion and MODIS. After calibration of the parameters, SAFY was run to simulate LAI, DAM, and yield. The steps of calibration in PSO were as follows.

1) The initial values (position) and velocity of each SAFY parameter to be calibrated were determined from previous studies.
2) SAFY was run using climate inputs and initial parameter values to obtain simulated LAI (hereafter S_{LAI}).
3) A cost function (c) was used to assess the discrepancy between S_{LAI} and F_{LAI} and M_{LAI} for every number (n) of available inputs between the beginning and end of simulation period (8).

$$C = \sqrt{\sum_{i=1}^{N} \left(\frac{(s_{\mathrm{LAI}} - F_{\mathrm{LAI}})}{F_{\mathrm{LAI}}} / N \right)}. \tag{8}$$

4) The best point of the ith particles and of all particles in the swarm was searched.
5) The position and velocity of particles were updated using the main model of the PSO.
6) Evaluate if the iteration target is reached, which was 30 based on [16]. If the iteration target reaches the final LAI, biomass and yield are simulated using the newly calibrated parameters.

E. Model Evaluation and Validation

We compared the performance of SAFY calibration using Landsat–MODIS fused and MODIS-derived LAI and phenology information with assimilation based on field data. The simulated model outputs were evaluated against ground-measured LAI, biomass, and yield in rice and maize sample fields. We evaluated the difference in the assimilation of LAI derived at Landsat (30 m) and MODIS (500 m) spatial resolution in capturing crop yield variability with the model calibrated using field data. We randomly selected 5% of the predicted yield pixels to compare the influence of MODIS and Landsat–MODIS fusion-derived phenological information in detecting spatial variability. R^2, RMSE, rRMSE and bias were used to evaluate the model

TABLE II
COMPARISON OF SAFY PARAMETERS CALIBRATION USING DATA FUSION AND MODIS-DERIVED LAI IN RICE AND MAIZE SAMPLE FIELDS

Crops	Calibration input	D_0 (DOY)	Pla	Plb	S_{TT} (^{0}c)	R_S (^{0}c)	ELUE (g.MJ^{-1})	RMSE	rRMSE (%)
Rice	Ground	198±5	0.29	0.0016	990±30	6575	2.30±0.19	0.4	26
	Fused	197±6	0.29	0.0016	947±85	6575	2.30±0.33	0.54	26
	MODIS	190±6	0.29	0.0016	889±96	6575	2.10±0.37	0.38	28
Maize	Ground	179±5	0.375	0.0015	729±95	6619	2.64±0.50	0.33	16
	Fused	175±3	0.375	0.0015	681±130	6619	2.75±0.46	0.44	17
	MODIS	167±11	0.375	0.0015	728±83	6619	2.62±0.36	0.49	22

performance. The influence of input and calibrated parameters in SAFY simulation was evaluated using sensitivity analysis. Sensitivity analysis was made after optimization of SAFY to analyze the influence of the three inputs (*Rg*, *Ta*, and LAI) and six sensitive parameters (Pla, Plb, S_{TT}, Rs, D_0, and ELUE) that drive SAFY outputs (LAI and yield) using a one-parameter at a time approach following Haan [42] in maize and rice samples. The inputs and parameters varied randomly 10 000 times between $\pm 2\sigma$ of mean values, while the other inputs and parameters were kept at their calibrated mean. After standardizing the variables and model outputs, we regressed the model output against the inputs. The slope of the relationship determines the weight of inputs and parameters on the model outputs.

IV. RESULTS

A. Calibration and Sensitivity Analysis

Table II presents the calibration accuracy of SAFY using field, fused, and MODIS data assimilation. The optimization was robust because the model was optimized within the maximum number of iterations set in this study (30) with a small calibration error. Field data assimilation provided the least error and good consistency of LAI simulation in relation to the calibrated LAI (RMSE = 0.33m^2/m^2, rRMSE = 16% for maize and RMSE = 0.40 m^2/m^2, rRMSE = 26% for rice) followed by data fusion (RMSE = 0.44 m^2/m^2, rRMSE = 17% for maize and RMSE = 0.54 m^2/m^2, rRMSE = 26% for rice) and MODIS (RMSE = 0.49 m^2/m^2, rRMSE = 22% for maize and RMSE = 0.38 m^2/m^2, rRMSE = 28% for rice). SAFY had better optimization accuracy in maize than in rice.

The calibrated D_0, S_{TT}, and ELUE had high standard deviations reflecting the field level variability of these parameters, while Pla, Plb, and Rs varied by crop type and were invariant by the calibration input sources. The phenological parameters ingested as inputs (D_0 and S_{TT}) showed higher standard deviations among sample fields and were influenced by the source of calibration inputs. Data fusion D_0 showed closer agreement with field D_0, and the MODIS determined D_0 was earlier than the field and the Landsat-MODIS fusion. Unlike data fusion, MODIS's short vegetative and growing season length resulted in smaller S_{TT} and R_S because the S_{TT} and R_S depend on accumulated *Ta* during the growing stages. Moreover, the source of calibration input influenced the value of ELUE, higher using fused (2.75 g.MJ^{-1} for maize and 2.3 g.MJ^{-1} for rice), field (2.64 g.MJ^{-1} for maize and 2.3 g.MJ^{-1} for rice) than MODIS (2.62 g.MJ^{-1} for maize and 2.1 g.MJ^{-1} for rice) data assimilations.

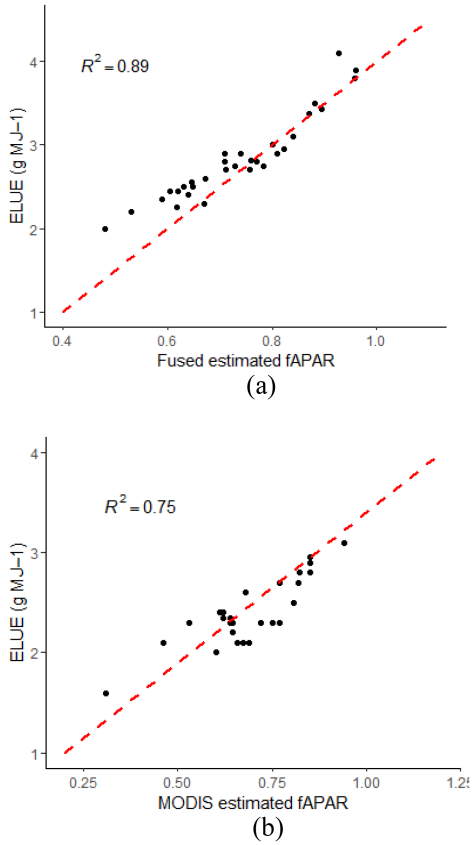

Fig. 4. Relationship of maximum fAPAR and calibrated ELUE using (a) data fusion and (b) MODIS assimilation.

TABLE III
SLOPE (B1), INTERCEPT (B0), AND COEFFICIENT OF DETERMINATION (R^2) OF A LINEAR FIT OF SAFY SIMULATED LAI AND YIELD VERSUS THE INPUTS AND CALIBRATED PARAMETERS

Inputs	Maize						Rice					
	LAI			Yield			LAI			Yield		
	B_0	B_1	R^2	B_0	B_1	R^2	B_0	B_1	R^2	B_0	B_1	R^2
Rg	-0.03	1.02	0.99	0.03	0.99	0.99	-0.09	1.02	0.98	-0.09	1.04	0.99
Ta	0.89	-0.95	0.98	1	-0.74	0.41	0.88	-0.95	0.98	1	-0.74	0.4
LAI				0.04	1.07	0.98				0.07	1.062	0.97
Parameters												
ELUE	-0.06	1.1	0.99	-0.37	1.33	0.95	-0.14	1.1	0.97	-0.21	1.14	0.94
D_0	0.26	0.81	0.94	0.56	0.51	0.22	0.23	0.89	0.93	0.47	0.7	0.69
Pla	0.76	-0.97	0.87	1.1	-0.89	0.67	0.64	-0.8	0.81	1	-0.82	0.66
Plb	0.67	-0.97	0.72	0.67	-0. 46	0.15	0.51	-0.83	0.56	0.4	-0.74	0.31
S_{TT}	0.39	0.85	0.79	0.19	0.6	0.33	0.13	0.84	0.94	-0.12	0.9	0.56
R_S	0.05	0.87	0.75	-0.11	0.83	0.67	0.06	0.89	0.95	-0.22	0.91	0.7

The inputs were perturbed 10 000 times between ±2σ, while others were fixed at their mean.

We also obtained a strong exponential relation between fused calibrated ELUE and ground fAPAR (see Fig. 4), reflecting data fusion provided more accurate field and crop-specific ELUE.

Table III shows that the climate inputs and calibrated parameters had a major influence on SAFY. Rg, LAI, and ELUE were the main factors influencing SAFY because they had the highest slope to LAI and crop yield simulations. LAI simulation was sensitive mainly to ELUE, Pla, Plb, and Rg, whereas Rg, ELUE, and LAI were the main determinants of SAFY yield simulation. SAFY showed sensitivity differences in rice and maize fields to Rg and phenological parameters determining the dynamics of

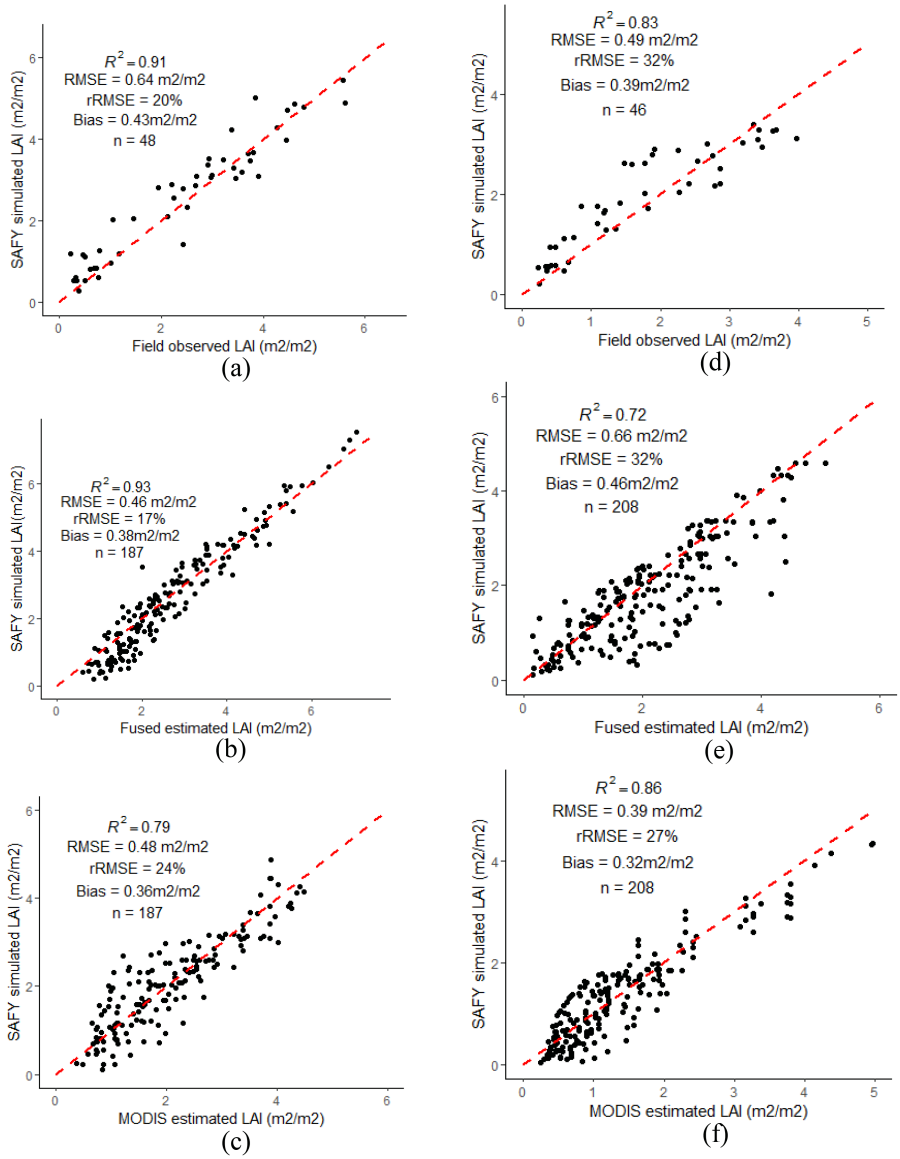

Fig. 5. Comparison between SAFY simulated LAI and field-measured LAI in (a) maize and (d) rice; data fusion LAI in (b) maize and (e) rice, and MODIS estimated LAI in (c) maize and (f) rice sample fields.

LAI (D_0, Pla, Plb, $S_{TT,}$ and R_S). For instance, the higher effect of Rg in rice yield than maize coincides with the METRA-2 bias compared to the ground measured Rg. The variation in the magnitude of maize and rice LAI during the growing season contributed to sensitivity variation to phenological parameters.

The source of LAI also showed a higher slope and sensitivity to SAFY yield simulation. However, as shown in Fig. 5, SAFY achieved good LAI simulation accuracy with F_{LAI} (b) and (e), field LAI (a) and (d), and M_{LAI} (c) and (f), indicating good model optimization accuracy. SAFY simulated LAI and the calibration LAI input correspondences when the model is run using data fusion and field data than MODIS. In maize fields, data fusion assimilation showed higher correspondence (rRMSE = 17%, $R^2 = 0.93$), followed by field data assimilation (rRMSE = 20%, $R^2 = 0.91$), and MODIS (rRMSE = 24%, $R^2 = 0.79$). MODIS retrieved LAI values were lower than the data fused retrieved, which influenced the SAFY simulation. Improved LAI simulation accuracy of data fusion over field data assimilation could be due to the increased frequency of LAI input. The three data sources did not show much difference in rice sample fields. However, compared to ground observation, MODIS underestimated rice LAI.

B. Biomass and Yield Estimation

1) *Biomass estimation:* Fig. 6 presents the progression of simulated LAI and DAM during the growing season. LAI and DAM capture the crops' phenological development well; showing SAFY could estimate crop productivity after the assimilation of EO data. The maximum increase in DAM is in accordance with the high photosynthetic activity at maximum LAI between DOY 225 to DOY 265

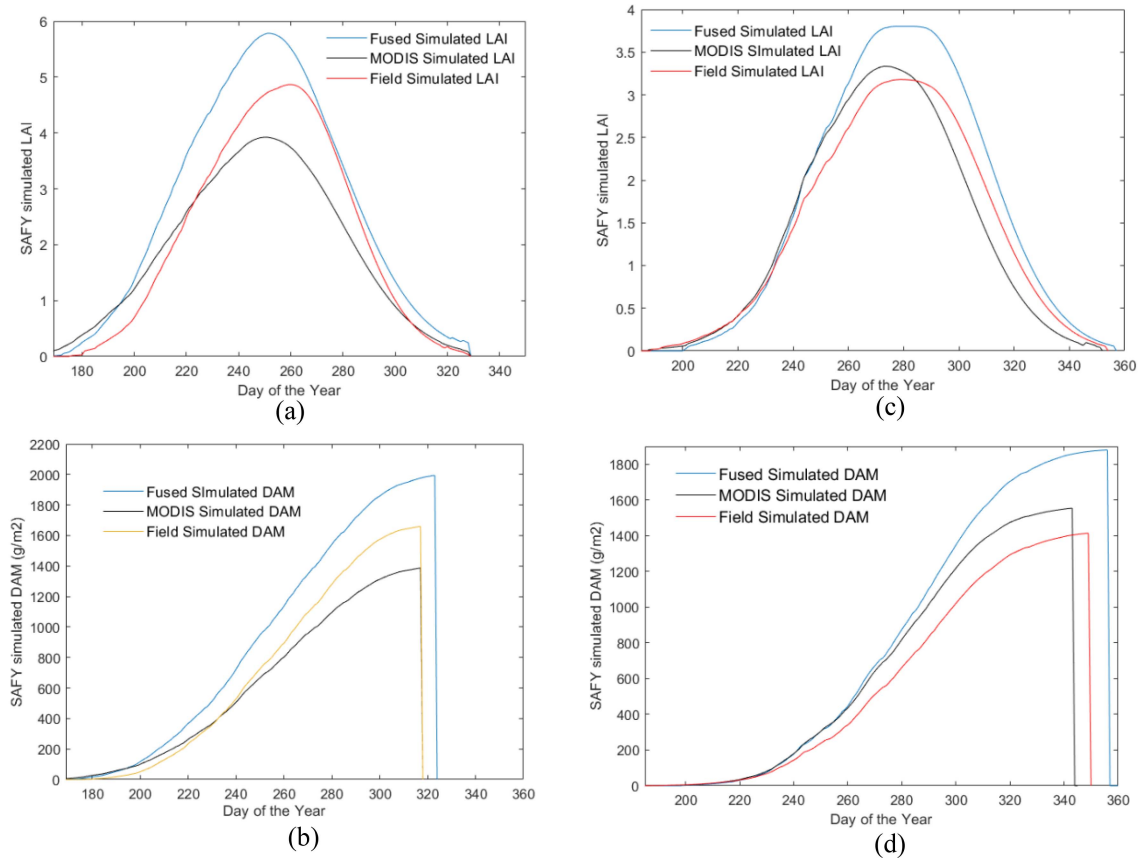

Fig. 6. Temporal evolution of the mean simulated LAI for (a) maize and (c) rice, and simulated DAM for (b) maize and (d) rice using fused, MODIS, and field data assimilation.

in maize fields and DOY 240 to DOY 290 in rice fields. After the greening period, the DAM growth rate increased significantly, and at peak growth stage (about 80 days after sowing (DAS) in maize and 95 DAS for rice), the DAM growth rate peaked. Biomass growth ended after the grain-filling stage (150 DAS for maize and 160 DAS for rice). On average, the simulated maize DAM was higher using data fusion (2000 g/m^2) than field (1600 g/m^2) and MODIS (1400 g/m^2) data assimilations. The lower value of DAM by MODIS could be associated with the lower amplitude of M_{LAI} input used for calibration. The steep slope in maize LAI coincides with higher DAM and the shallow slope in rice exhibited lower leaf allocation to DAM.

2) *Crop yield estimation:* Fig. 7 shows SAFY estimated maize and rice yield using field, fused, and MODIS data assimilations was comparable to in situ measured yield. On average, data fusion estimated maize (778 $\pm$ 236 g/m^2) and rice (392 $\pm$ 131 g/m^2) yield compared with the mean measured yield in maize (781 $\pm$ 129 g/m^2) and rice (366 $\pm$ 141 g/m^2) sample fields. SAFY based on data fusion showed lower maize estimation error (rRMSE = 16%) followed by field (rRMSE = 17%) and MODIS (rRMSE = 20%) data assimilation. In rice, data fusion showed lower estimation error (rRMSE = 23%) than field (rRMSE = 25%) and MODIS (rRMSE = 35%) assimilation. The 1:1 regression line between simulated and measured yield also indicates that SAFY underestimated crop yields and the scatter of points indicates that data fusion captured field-level yield variability well. As shown in Table III, Rg, LAI, and ELUE were the main determinants of SAFY yield that contributed to yield estimation performance variation by the source of calibration inputs. High sensitivity of SAFY to the LAI input and the more accurate LAI retrieval from data fusion (see supplementary material, Fig. S2) improved the yield estimation accuracy of data fusion than MODIS. SAFY performed better in maize than rice fields, regardless of the sources of assimilation. The higher LAI estimation error in rice fields than in maize could contributed to accuracy variation. Good model calibration accuracy (see Table II), unlike the low yield estimation performance in rice, can be associated with the error in the grain partitioning parameters and field measurement uncertainty.

C. Spatial Distribution of Crop Yield Estimation

Fig. 8 shows that both Landsat–MODIS fusion (a) and MODIS (b) data assimilations were able to map the spatial variation of yield estimation. Data fusion estimated a higher

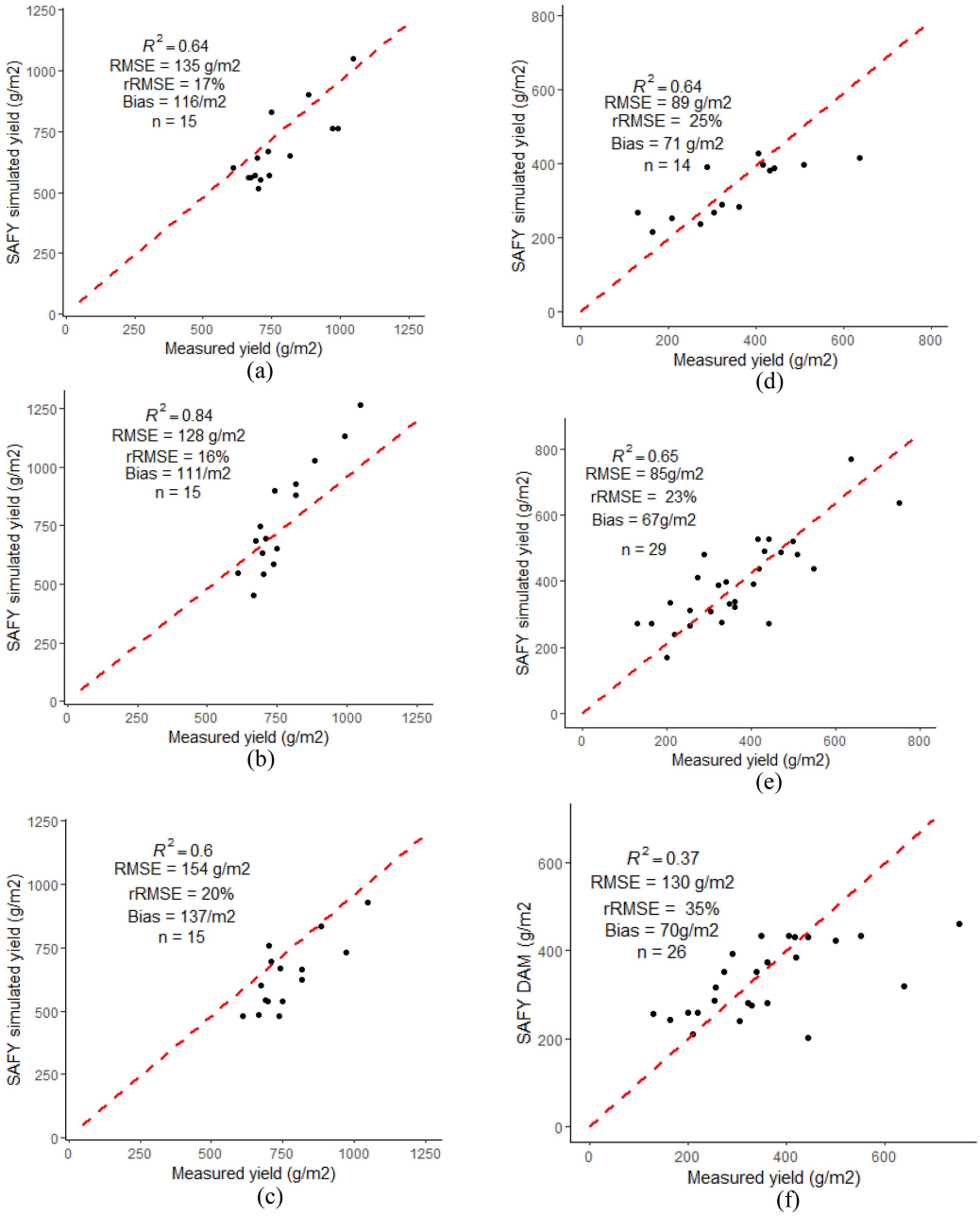

Fig. 7. Comparison between measured and simulated yield in maize using (a) field, (b) data fusion, and (c) MODIS, and rice fields using (d) field, (e) data fusion and (f) MODIS assimilations.

mean yield (683 $\pm$ 111 g/m^2 for maize and 497 $\pm$ 134 g/m^2 for rice) than MODIS (566 $\pm$ 76 g/m^2 for maize and 496 $\pm$ 170 g/m^2 for rice), consistent with the validation result (see Fig. 7). The spatial variation and the difference between data fusion and MODIS coincide with the spatial distribution of crops and their growing environment. For instance, the maize dominant (south of Lake Tana) had the highest yield value ($\geq$ 700 g/m^2) than rice (Fogera) site (400—600 g/m^2). In the highlands, where fields are small and crops are mixed (Dangla, South Mecha, and Bahir Dar Zuriya), the estimated yield was lower than in the mechanized farming site in Koga. The zoom windows show that data fusion better captured pixel level crop yield variability than MODIS.

D. Factors Influencing Spatial Variability of Yield

Fig. 9 shows that the input LAI and ELUE were the most important predictors of SAFY yield and the main factors for field/pixel-level yield variability. SAFY estimated yield showed a higher correlation with LAI and ELUE when the model was run using fused data than MODIS. Thus, consistent with the sensitivity analysis result, field-level calibration of ELUE using data fusion-derived LAI contributed to better estimation of crop yield. LAI-yield relation was also stronger with data fusion (a) than MODIS (b) assimilations, possibly due to the high spatial resolution capturing small crop fields. As shown in the subsets

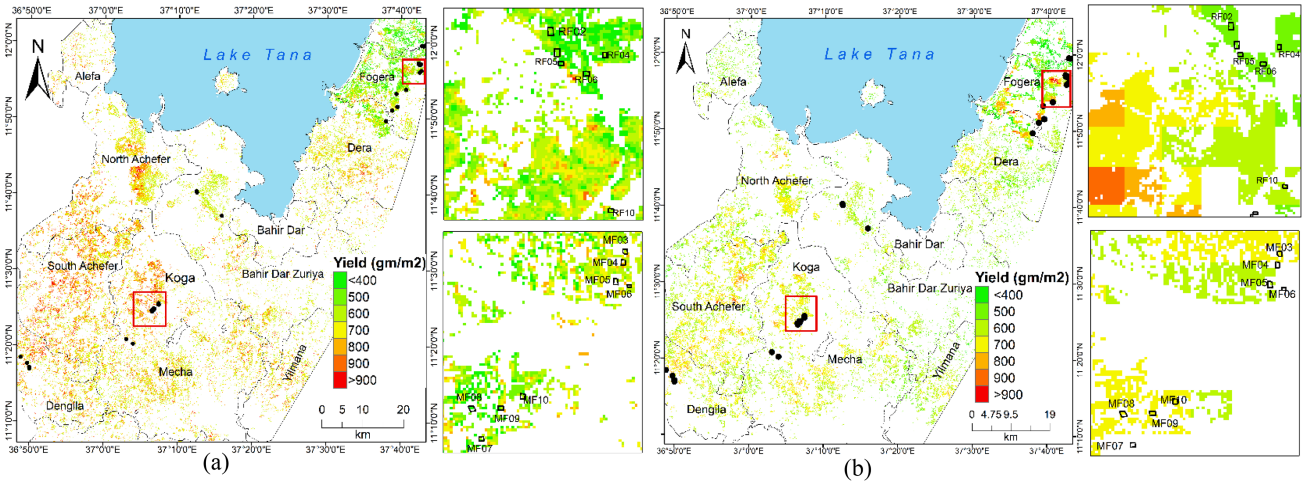

Fig. 8. Spatial distribution of crop yield map using (a) Landsat—MODIS fusion and (b) MODIS data assimilations

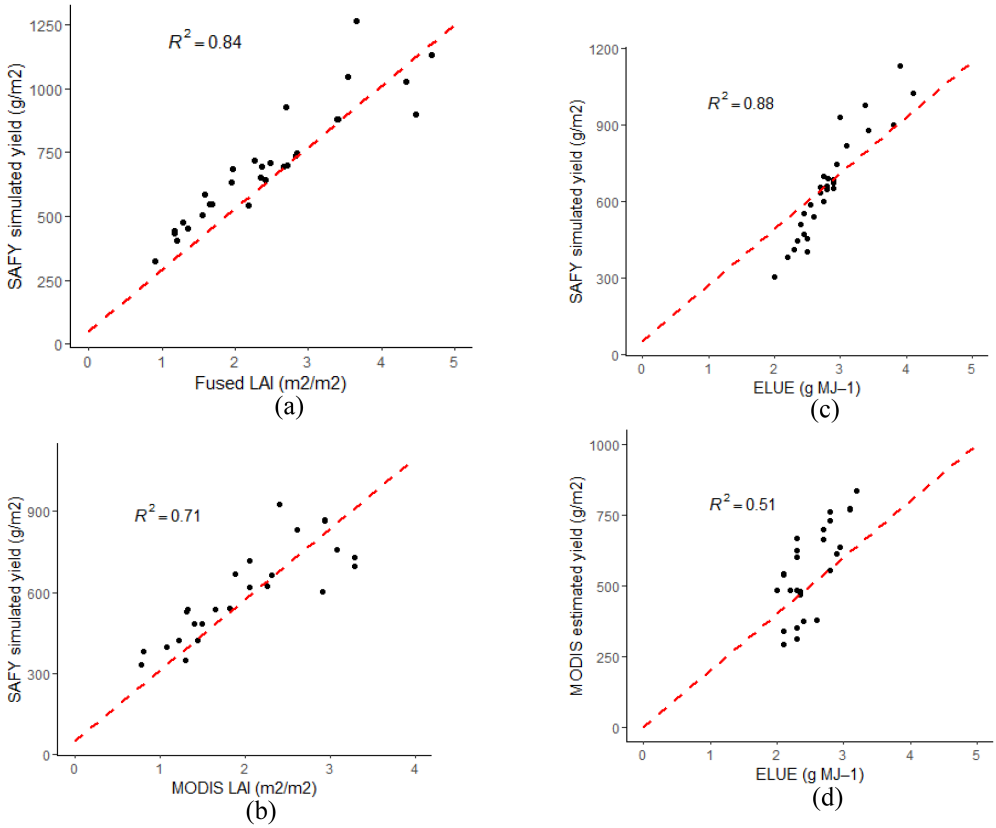

Fig. 9. Correlation of SAFY simulated yield with maximum LAI derived from (a) data fusion, (b) MODIS and with (c) data fusion and (d) MODIS calibrated ELUE on maize and rice sample fields.

in Fig. 8, the footprint of sample fields' mean LAI (60 m) is represented by about two Landsat pixels, where MODIS could not distinguish crop fields. Moreover, the 1:1 line using data fusion [see Fig. 9(c) and (d)] suggests pixel-level calibration of ELUE captures the management and environmental drivers of crop growth variation among smallholder farmers.

Fig. 10 shows the effects of phenology information determined from data fusion and MODIS in crop yield estimates. An earlier emergence (days before DOY 175) produced a higher maize yield estimation than a late emergence date (days after DOY 180) when the model was run using fused data (a). However, early emergence date detection with MODIS did not

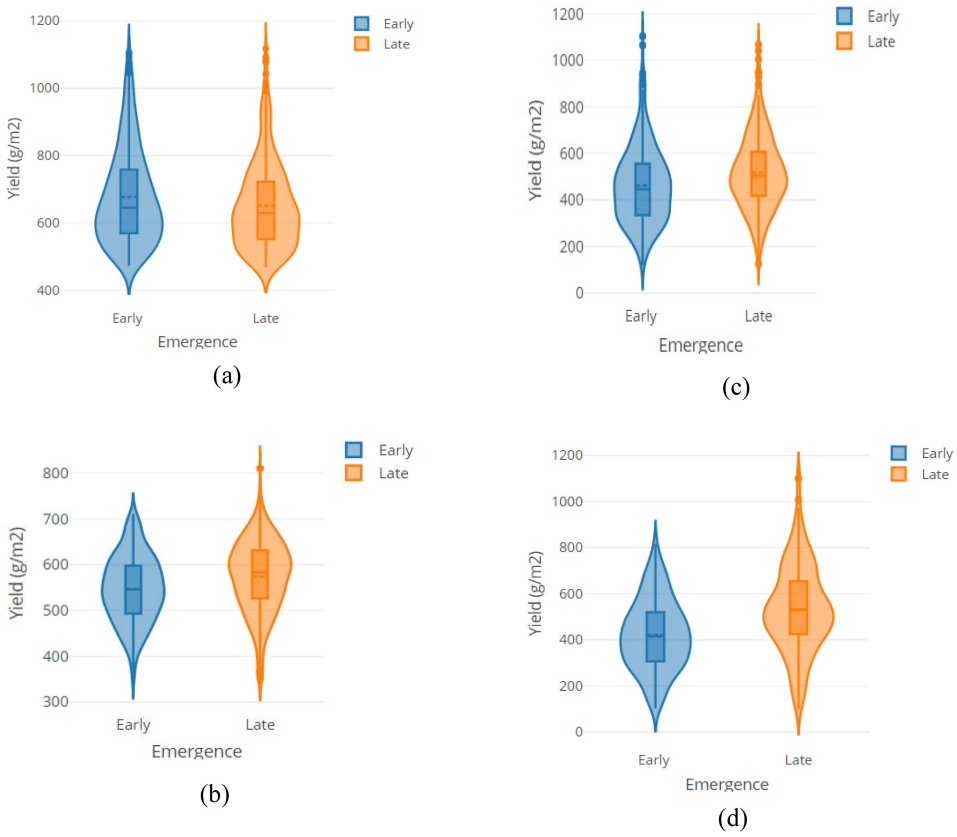

Fig. 10. Violin plot showing the distribution of crop yield to pixels showing early and late phenology detection from data fusion in (a) maize and (c) rice and MODIS in (b) maize and (d) rice for 5% of the cropland pixels.

contribute to high maize yield estimation because the grain filling occurred when the incoming radiation was lower (August to early September), resulting in a lower yield estimate. The late MODIS D0 contributed more to higher maize (b) and rice (d) yields than early D0. Early D0 from data fusion in maize (a) estimated a higher yield, possibly because of less moisture stress during the grain filling period (September to October) caused by the early end of the rainy season. Water stress was not an issue for rice due to abundant soil moisture in the rice-growing floodplain, and pixels with late D0 (after DOY 205) produced a higher yield than pixels with early D0 (DOY before 195) in both MODIS and data fusion assimilations. Late D0, after the progress of the rainy season (mid-July), could also contribute to an increase in the water volume in the early rice growth stage.

V. Discussion

Our study addressed a major obstacle in agricultural research: the field-level data requirements of crop growth models and the spatial and temporal mismatch of EO data. Assimilating Landsat–MODIS fused data in a semiempirical model, meets the high spatial resolution and temporal resolution input requirements to improve field-level yield estimation in smallholder agricultural systems in Africa. We assimilated LAI and phenology information derived from fused (30 m), MODIS (500 m), and field data in SAFY for comparison. The main findings of the study were as follows:

1) field and environment-specific parameters of SAFY (D_0, S_{TT}, and ELUE) were influenced by the source of calibration input, unlike the crop-specific parameters (Pla, Plb, and R_S);
2) improved LAI and phenology estimation accuracy through data fusion increased calibration and yield estimation accuracy of the model;
3) late end of season detection using data fusion was associated with higher estimated yield, while an early start of season detection with MODIS resulted in lower estimated yield;
4) yield estimation performance showed variation by crop type, and was higher in maize than rice and according to the environment.

Our results revealed that calibration using Landsat–MODIS fusion increased crop yield estimation accuracy and captured spatial variability in yield in smallholder farm fields, which is crucial for crop production and food security monitoring.

A. Assimilation of LAI and Phenology Information in SAFY

SAFY was sensitive to the Rg, LAI inputs and the parameters determining the dynamics of LAI and yield (Pla, Plb, Rs, D_0, S_{TT}, and ELUE). The calibrated Pla, Plb, and Rs parameters

varied by crop type (rice and maize) and did not vary at the field level and by the source of LAI input for calibration. Our results contradicted [20] and [22], who argued that all these parameters are field-specific and their value changes when calibrated with different EO data sources. We fixed the growing season length using phenological dates detected from EO. The field-level variation of the model outputs was controlled by field-to-field calibration of the ELUE and the phenology parameters (D_0 and S_{TT}). Unlike the findings by [21], we found a higher standard deviation of S_{TT} (133 °C), suggesting S_{TT} is a field-specific parameter because of the large management (sowing date, fertilizer application, and weed control) and environmental factors (weather, soil fertility, and topography) variation in our area. Moreover, the strong correlation of the most sensitive parameter of SAFY (ELUE) with the maximum fAPAR indicates the possibility of effectively estimating it from EO data, which minimizes the computational cost during field-level calibration, consistent with previous studies [10], [22]. Therefore, assimilation of EO data in the crop growth model contributed to obtain the field-level parameters, which is important for large area crop yield estimation in data scarce regions in Africa.

B. Crop Yield Estimation

The overall yield estimation accuracy of SAFY increased when the model was calibrated with data fusion and field data rather than MODIS assimilation. Compared to the in situ measurement, data fusion provided lower yield estimation error (rRMSE = 16% for maize and rRMSE = 23% in rice) than field data (rRMSE = 17% for maize and rRMSE = 25% in rice) and MODIS (rRMSE = 20% for maize and rRMSE = 35% in rice) assimilations. Our yield estimations using data fusion assimilation for maize (7 t/ha) and rice (4.4 t/ha) agree with observations by [2] in the study area. Assimilation of fused data in SAFY model captured the large yield variability of the smallholder farms in the study area, which is important for large-area applications. The growth of multiple crops with similar phenology and difficulties in obtaining field-level information are the main challenges for the lack of reliable yield estimation in most smallholder systems across Africa [4]. We obtained frequent observation (8-days) through data fusion at 30-m spatial resolution to determine phenological parameters and the continuous LAI improved the model yield estimation accuracy. Calibrating the field and crop-specific parameters at MODIS spatial resolution could lead to uncertainty due to the mix of other vegetation classes in smallholder agricultural systems [17], [43]. For instance, Gao et al. [8] reported that even if MODIS (250 m) captures yield variability in relatively homogeneous agricultural landscapes in Central Iowa, USA, yield estimation still improved when MODIS was fused with Landsat. It was also not feasible to obtain field-level information using ground measurement for the important model variables (LAI, D_0, and ELUE), which limits the applicability of field data assimilation. Yield estimation performance difference between fused and field in our study was related to the number of LAI observations $n = 3$—4 in field data and $n = 14$ for data fusion assimilations. Precise determination of model parameters such as ELUE was attained when the model was calibrated using frequent data fusion observations, consistent with [10]. However, a recent study [14] indicated that a higher weight for assimilation of jointing and anthesis stages LAI improved wheat yield in the WOFSOT model and acceptable yield estimation has been reported with observations between booting and heading stages [15], which can be investigated and considered when observations are limited.

The source of calibration LAI input influenced crop yield prediction performance. The higher deviation of LAI, DAM, and yield simulated based on MODIS compared to ground data was associated with the empirical model to estimate LAI. This finding is similar with [25] and [44], in which under and overestimation in SAFY is attributed to the accuracy of EO-estimated LAI. Data fusion estimated higher LAI than MODIS in rice and maize fields, which resulted in a higher estimated yield value using data fusion. Data fusion's ability to capture small crop fields improved the LAI estimation accuracy more than MODIS. For instance, the footprint of our ground LAI measurement at the farm field scale (60 m × 60 m), which better coincides with the LAI retrieved from Landsat than from MODIS, influenced the crop yield estimated. Yield estimation accuracy generally decreased when the spatial resolution decreased from 30 to 500 m. In the small and irregular farm fields, however, data fusion algorithms could result in the loss of spectral information of the target crops [11]. In this regard, Dong et al. [9] indicated that LAI estimated from fused data showed a slight deviation from LAI derived from the actual image. Similar pixel selection is the most important step in deriving the relationship between the high-resolution and coarse-resolution inputs in data fusion. We integrated a land cover map to improve similar pixel selection to capture reflectance change in the fragmented agricultural landscape. Therefore, the Landsat–MODIS fusion maize and rice LAI estimates showed more consistency with field measurements than MODIS [12]. Nevertheless, data fusion uncertainties and cloud cover are still potential challenges to use optical remote sensing in yield estimation in Africa. As a result, there is a growing interest in integrating synthetic aperture radar (SAR) and optical remote sensing for crop growth monitoring and yield estimation [14], [20] that could be further investigated in smallholder agricultural systems.

Phenological parameters derived from data fusion improved the SAFY simulation. Phenology is an important parameter in crop growth models, which are usually unavailable at the required spatial scale and accuracy in smallholder farms [22]. Relatively accurate phenology parameters from Landsat–MODIS fusion, consistent with ground sowing and harvest date information [12], contributed to improved crop yield estimation. Studies also reported that accurate crop phenology detection from EO is important in crop modeling because phenology controls crop biomass distribution [17], [25], [37]. Moreover, optimizing SAFY using EO-derived phenology reduced yield estimation uncertainty due to the use of generalized regional crop calendar information. Hence, integrating EO-derived phenology information minimized model uncertainty and contributed to capturing the large management and environmental variation in smallholder farms.

The length of the growing season detected by data fusion and MODIS contributed to yield estimation variation of fused and MODIS data assimilations. Because the timing of phenological parameters (D_0, S_{TT}, and R_S) determines the magnitude of simulated LAI, the length of the season and the partitioning to yield, consistent with the findings in [17]. The longer growing season detected by data fusion means a more extended grain filling period and a higher DAM and yield estimation, while the short growing length season from MODIS means a short grain filling period and quick senescence (small S_{TT} and R_S), resulting in lower yield. We also observed that pixels with early D_0 estimated low yield, probably because crops with short growing season lengths absorb less PAR, as confirmed by [17]. The result agrees with Kang and Özdoğan [35], who found that phenological shift causes a significant reduction in estimated yield.

Biomass and yield prediction accuracy was higher in maize than in rice, regardless of the source of data assimilations. The first possible reason could be the uncertainty of the fixed parameters. Unlike rice, we obtained various maize experiments based on SAFY and other light efficiency-based models to parameterize the fixed parameters [19], [22], [40]. Although the calibration accuracy of rice was good, we found a higher DAM and yield error, implying that the fixed parameters influencing biomass and yield portioning (DAM_0 and HI) contributed to the error. It was also reported that SAFY performs poorly when yield is greatly limited by stress due to weeds, pests, and diseases [45]. Although weeds are a common problem, the higher sensitivity of rice to weeds than maize could be the second reason for SAFY's low performance in rice. The third reason for the high yield estimation error using data fusion in rice could be the data fusion error. Validation of the modified ESTARFM showed higher data fusion error in rice fields because of the large spatial variation of phenology during the vegetative stage, influencing similar pixel selection when the Landsat input was far from the prediction date [12]. The difficulty of obtaining pure and homogeneous pixels in the small agricultural field and the lack of frequent cloud-free Landsat input could result in data fusion uncertainty and yield estimation error.

SAFY generally underestimated crop yield compared to ground observation regardless of the inputs used for calibration, and MODIS underestimation was larger than field and data fusion assimilations. We found a strong correlation between simulated crop yield and peak growth stage LAI, indicating that yield estimation error was not due to calibration error [35]. Moreover, we only calibrated four parameters of SAFY (Pla, Plb, RS, and ELUE), and the errors were not due to the calibration of several sensitive parameters [20]. Therefore, the source of error could be associated with ground measurement errors and model uncertainty. The higher DAM error in all three sources of calibration inputs implies SAFY simulation error could be due to field measurement error resulting from the high within-field crop growth variability. Moreover, the simplicity of SAFY to estimate DAM as a function of photosynthetically active radiation could also be the source of uncertainty. Studies pointed out that SAFY has a poor capability of correlating LAI compared to complex crop models [25], [44]. Alternatively, studies indicated that machine learning approaches effectively estimate crop yield from EO data [5], [46]. Zhao et al. [23] showed that machine learning approach (RMSE of 1.13 t ha^{-1} and R^2 of 0.47) and SAFY (RMSE of 1.33 t ha^{-1} and R^2 of 0.46) provided similar results. The authors also showed that SAFY has been integrated with machine learning methods to simulate the large number of training sample input requirements of machine learning approaches. Therefore, machine learning and a hybrid method integrating learning methods with simple crop models such as SAFY can be potential approaches to estimate crop yield every growing season in smallholder systems in Africa, which is an important research outlook.

C. Spatial Variability of Yield Estimation

Field-level calibration of ELUE and integration of phenological parameters determined from data fusion contributed to detecting spatial variation of yield estimates. The spatial variation coincides with the crop type distribution, higher in maize than rice; and with management practice, higher in mechanized farming and lower in the mixed crop and fragmented locations. The large spatial variation of D_0 and S_{TT}, which correspond to the large sowing date and management practice variations of smallholder farmers, contributed to the spatial variation of yield estimate. The strong correlation of ELUE with crop yield ($R^2 = 0.95$) implies that ELUE was the main factor for spatial variability of crop yield because ELUE accounts for yield-limiting factors such as water and nutrient stress in SAFY [35]. Our result confirms that including water balance in the SAFY model is unnecessary as long as ELUE is calibrated with EO-derived LAI [19], [37]. However, stress factors during the grain filling stage, such as high temperature, pests, and disease, could also lead to discrepancies between calibration and yield prediction accuracy [45]. Thus, joint assimilation of parameters that determine yield (e.g., soil moisture) and integration of yield in the calibration process could further improve yield prediction, which is worth further investigation.

In general, the major contribution of our study is the assimilation of LAI and phenology information determined from Landsat–MODIS fusion to capture the spatial variation of crop yield in smallholder agricultural systems, which could contribute to crop production monitoring. Silvestro et al. [16] showed that despite the smaller number of parameters, SAFY provided more accurate yield estimation than the AquaCrop model and estimated comparable results with the complex crop models [23]. SAFY has been proven effective in yield estimation for various crops in previous studies, but to our knowledge, this is the first to test the model in rice and a highly fragmented tropical agricultural landscape in Africa. In light of the promising results, it is important to address the sources of model uncertainty and test the transferability of the model in space and time for large-area applications.

VI. Conclusion

The large input requirements of crop growth models and the prevalence of fragmented landscapes are fundamental challenges of crop yield estimation in sub-Saharan Africa. The

study calibrated a semiempirical model (SAFY) using EO data to improve crop yield estimation in a smallholder agricultural landscape in Ethiopia. We used a fusion of Landsat and MODIS data to meet the high spatial and temporal resolution EO data requirements of SAFY. LAI and phenology information estimated from Landsat–MODIS fusion was assimilated, and the result was compared to MODIS and field data assimilations. Validation using ground data showed that data fusion assimilation provided more accurate field-level yield estimation due to its phenology and LAI estimation accuracy.

Among the sensitive parameters of SAFY, D_0, S_{TT}, and ELUE were crop and field-specific and influenced by the source of calibration inputs. Data fusion contributed to the accurate calibration of the crop and field-specific parameters, which capture the spatial variability of crop yield. Moreover, we obtained smaller LAI, DAM, and yield estimation errors compared to ground measurement when using data fusion than using MODIS because data fusion detected the small crop fields of the study area. Although field data assimilation provided good yield estimation, it is inapplicable for large-area estimates. The improved yield estimation performance using data fusion in fragmented agricultural landscapes could be a valuable input for crop production monitoring and food security analysis.

ACKNOWLEDGMENT

The authors would like to thank the developers of SAFY (Dr. B. Duchemin) and ESTARFM (Dr. X. Zhu) for providing their codes to be used in this study, and the NASA Land Processes Distributed Active Archive Center (LP DAAC) and US Geological Survey (USGS) for sharing MODIS and Landsat data. The authors would also like to thank farmers in the study area for allowing field data collection in their farm fields.

REFERENCES

[1] M. Burke and D. B. Lobell, "Satellite-based assessment of yield variation and its determinants in smallholder African systems," *Proc. Nat. Acad. Sci. USA*, vol. 114, no. 9, pp. 2189–2194, 2017.

[2] D. T. Meshesha and M. Abeje, "Developing crop yield forecasting models for four major Ethiopian agricultural commodities," *Remote Sens. Appl., Soc. Environ.*, vol. 11, pp. 83–93, 2018.

[3] Z. Jin et al., "Mapping smallholder yield heterogeneity at multiple scales in Eastern Africa," *Remote Sens.*, vol. 9, no. 9, 2017, Art. no. 931.

[4] D. B. Lobell, "The use of satellite data for crop yield gap analysis," *Field Crops Res.*, vol. 143, pp. 56–64, 2013.

[5] M. Marshall et al., "Field-level crop yield estimation with PRISMA and Sentinel-2," *ISPRS J. Photogrammetry Remote Sens.*, vol. 187, pp. 191–210, 2022.

[6] A. K. Whitcraft et al., "Meeting Earth observation requirements for global agricultural monitoring: An evaluation of the revisit capabilities of current and planned moderate resolution optical Earth observing missions," *Remote Sens.*, vol. 7, no. 2, pp. 1482–1503, 2015.

[7] P. C. Doraiswamy et al., "Application of MODIS derived parameters for regional crop yield assessment," *Remote Sens. Environ.*, vol. 97, no. 2, pp. 192–202, 2005.

[8] F. Gao et al., "Assessing the variability of corn and soybean yields in central Iowa using high spatiotemporal resolution multi-satellite imagery," *Remote Sens.*, vol. 10, no. 9, Sep. 2018, Art. no. 1489.

[9] T. F. Dong et al., "Estimating winter wheat biomass by assimilating leaf area index derived from fusion of Landsat-8 and MODIS data," *Int. J. Appl. Earth Observ. Geoinf.*, vol. 49, pp. 63–74, Jul. 2016.

[10] T. F. Dong et al., "Estimating crop biomass using leaf area index derived from Landsat 8 and Sentinel-2 data," *ISPRS J. Photogrammetry Remote Sens.*, vol. 168, pp. 236–250, Oct. 2020.

[11] X. L. Zhu et al., "An enhanced spatial and temporal adaptive reflectance fusion model for complex heterogeneous regions," *Remote Sens. Environ.*, vol. 114, no. 11, pp. 2610–2623, Nov. 2010.

[12] B. Sisheber et al., "Tracking crop phenology in a highly dynamic landscape with knowledge-based Landsat–MODIS data fusion," *Int. J. Appl. Earth Observ. Geoinf.*, vol. 106, 2022, Art. no. 102670.

[13] S. Wu et al., "Regional winter wheat yield estimation based on the WOFOST model and a novel VW-4DEnSRF assimilation algorithm," *Remote Sens. Environ.*, vol. 255, 2021, Art. no. 112276.

[14] S. Wu, J. Ren, Z. Chen, P. Yang, H. Li, and J. Liu, "Evaluation of winter wheat yield simulation based on assimilating LAI retrieved from networked optical and SAR remotely sensed images into the WOFOST model," *IEEE Trans. Geosci. Remote Sens.*, vol. 59, no. 11, pp. 9071–9085, Nov. 2021.

[15] H. Li et al., "Improving winter wheat yield estimation from the CERES-wheat model to assimilate leaf area index with different assimilation methods and spatio-temporal scales," *Remote Sens.*, vol. 9, no. 3, pp. 190, 2017.

[16] P. C. Silvestro et al., "Estimating wheat yield in China at the field and district scale from the assimilation of satellite data into the aquacrop and simple algorithm for yield (SAFY) models," *Remote Sens.*, vol. 9, no. 5, pp. 24, May 2017.

[17] C. Liao et al., "Using spatio-temporal fusion of Landsat-8 and MODIS data to derive phenology, biomass and yield estimates for corn and soybean," *Sci. Total Environ.*, vol. 650, no. Pt 2, pp. 1707–1721, 2019.

[18] J. L. Monteith, "Solar-radiation and productivity in tropical ecosystems," *J. Appl. Ecol.*, vol. 9, no. 3, pp. 747–766, 1972.

[19] M. Claverie et al., "Maize and sunflower biomass estimation in southwest France using high spatial and temporal resolution remote sensing data," *Remote Sens. Environ.*, vol. 124, pp. 844–857, Sep. 2012.

[20] J. Betbeder, R. Fieuzal, and F. Baup, "Assimilation of LAI and dry biomass data from optical and SAR images into an agro-meteorological model to estimate soybean yield," *IEEE J. Sel. Topics Appl. Earth Observ. Remote Sens.*, vol. 9, no. 6, pp. 2540–2553, Jun. 2016.

[21] B. Duchemin et al., "A simple algorithm for yield estimates: Evaluation for semi-arid irrigated winter wheat monitored with green leaf area index," *Environ. Model. Softw.*, vol. 23, no. 7, pp. 876–892, 2008.

[22] M. Battude et al., "Estimating maize biomass and yield over large areas using high spatial and temporal resolution Sentinel-2 like remote sensing data," *Remote Sens. Environ.*, vol. 184, pp. 668–681, Oct. 2016.

[23] Y. Zhao et al., "Transfer-learning-based approach for yield prediction of winter wheat from planet data and SAFY model," *Remote Sens.*, vol. 14, no. 21, 2022, Art. no. 5474.

[24] S. Gummadi et al., "Spatio-temporal variability and trends of precipitation and extreme rainfall events in Ethiopia in 1980-2010," *Theor. Appl. Climatol.*, vol. 134, no. 3-4, pp. 1315–1328, Nov. 2018.

[25] C. Ma et al., "Wheat growth monitoring and yield estimation based on remote sensing data assimilation into the SAFY crop growth model," *Sci. Rep.*, vol. 12, no. 1, pp. 5473, 2022.

[26] S. J. Maas, "Parameterized model of gramineous crop Growth 1. Leaf-area and dry mass simulation," *Agronomy J.*, vol. 85, no. 2, pp. 348–353, Mar./Apr. 1993.

[27] M. Marshall and P. Thenkabail, "Developing in situ non-destructive estimates of crop biomass to address issues of scale in remote sensing," *Remote Sens.*, vol. 7, no. 1, pp. 808–835, Jan. 2015.

[28] D. K. Bolton and M. A. Friedl, "Forecasting crop yield using remotely sensed vegetation indices and crop phenology metrics," *Agricultural Forest Meteorol.*, vol. 173, pp. 74–84, 2013.

[29] F. Gao et al., "Fusing Landsat and MODIS data for vegetation monitoring," *IEEE Geosci. Remote Sens. Mag.*, vol. 3, no. 3, pp. 47–60, Sep. 2015.

[30] A. Huete et al., "Overview of the radiometric and biophysical performance of the MODIS vegetation indices," *Remote Sens. Environ.*, vol. 83, no. 1-2, pp. 195–213, Nov. 2002.

[31] Y. J. Yang et al., "Characterizing spatiotemporal patterns of crop phenology across North America during 2000-2016 using satellite imagery and agricultural survey data," *ISPRS J. Photogrammetry Remote Sens.*, vol. 170, pp. 156–173, Dec. 2020.

[32] L. Eklundh and P. Jönsson, *TIMESAT 3.3 With Seasonal Trend Decomposition and Parallel Processing Software Manual*, Lund Univ., Lund, Sweden, p. 92, 2017. [Online]. Available: https://www.nateko.lu.se/TIMESAT/

[33] T. Dong et al., "Deriving maximum light use efficiency from crop growth model and satellite data to improve crop biomass estimation," *IEEE J. Sel. Topics Appl. Earth Observ. Remote Sens.*, vol. 10, no. 1, pp. 104–117, Jan. 2017.

[34] X. L. Jin et al., "A review of data assimilation of remote sensing and crop models," *Eur. J. Agronomy*, vol. 92, pp. 141–152, Jan. 2018.

[35] Y. Kang and M. Özdoğan, "Field-level crop yield mapping with Landsat using a hierarchical data assimilation approach," *Remote Sens. Environ.*, vol. 228, pp. 144–163, 2019.
[36] D. V. Gaso, A. G. Berger, and V. S. Ciganda, "Predicting wheat grain yield and spatial variability at field scale using a simple regression or a crop model in conjunction with Landsat images," *Comput. Electron. Agriculture*, vol. 159, pp. 75–83, 2019.
[37] P. C. Silvestro et al., "Sensitivity analysis of the Aquacrop and SAFYE crop models for the assessment of water limited winter wheat yield in regional scale applications," *PLoS One*, vol. 12, no. 11, 2017, Art. no. e0187485.
[38] R. Confalonieri, A. S. Rosenmund, and B. Baruth, "An improved model to simulate rice yield," *Agronomy Sustain. Develop.*, vol. 29, no. 3, pp. 463–474, 2009.
[39] B. Sánchez, A. Rasmussen, and J. R. Porter, "Temperatures and the growth and development of maize and rice: A review," *Glob. Change Biol.*, vol. 20, no. 2, pp. 408–417, 2014.
[40] A. K. Srivastava et al., "Options for sustainable intensification of maize production in Ethiopia," *Sustainability*, vol. 11, no. 6, 2019, Art. no. 1707.
[41] R. Confalonieri et al., "Comparison of sensitivity analysis techniques: A case study with the rice model WARM," *Ecological Model.*, vol. 221, no. 16, pp. 1897–1906, 2010.
[42] C. T. Haan, *Statistical Methods in Hydrology*, 2nd ed. Ames, IA, USA: Iowa State Univ. Press, 2002.
[43] J. Huang et al., "Assimilation of remote sensing into crop growth models: Current status and perspectives," *Agricultural Forest Meteorol.*, vol. 276-277, 2019, Art. no. 107609.
[44] X. Peng et al., "Assimilation of LAI derived from UAV multispectral data into the SAFY model to estimate maize yield," *Remote Sens.*, vol. 13, no. 6, 2021, Art. no. 1094.
[45] S. Pignatti et al., "Sino-EU Earth observation data to support the monitoring and management of agricultural resources," *Remote Sens.*, vol. 13, no. 15, Aug. 2021, Art. no. 26.
[46] A. Kaneko et al., "Deep learning for crop yield prediction in Africa,".

Biniam Sisheber was born in Markos, Ethiopia, in 1983. He received the B.Sc. degree in geography and environmental studies from the Haromaya University, Dire Dawa, Ethiopia, in 2004, the M.S. degree in geographic information systems (GIS) and remote sensing from Addis Ababa University, Addis Ababa, Ethiopia. He is currently working toward the Ph.D. degree in natural resource management with the Faculty of Geo-information Science and Earth Observation (ITC), University of Twente, Enschede, The Netherlands.

His research interest includes application of remote sensing in agriculture and other natural resources.

Michael Marshall received the M.A. degree in environmental science & policy from Clark University, Worcester, MA, USA, in 2005, and the Ph.D. degree in geography from the University of California-Santa Barbara, California, USA, in 2010. He is an Associate Professor with the Faculty of Geo-Information Science and Earth Observation (ITC), University of Twente, Enschede, The Netherlands. His research interests include developing empirical or semiempirical models that integrate ground-based, Earth observation, and other geospatial data in a geographic information system to understand how agroecosystems impact the environment and Earth system.

Daniel Mengistu received the M.Sc. degree in land resource management and the Ph.D. degree in environment and natural resource management from Addis Ababa University, Ethiopia, in 2005 and 2015, respectively. He is an Associate Professor with Bahir Dar University, Bahir Dar, Ethiopia. His research interests include applications of remote sensing and geographic information system in hydrology, land use, and climate change modelling.

Andrew Nelson received the bachelor degree in civil engineering from Nottingham University, Nottingham, U. K., in 1994, and the M.Sc. degree in geographic information systems from the University of Leicester, Leicester, U.K., in 1997, and Ph.D. degree in geography from the University of Leeds, U.K., in 2004.

He worked with World Bank, Washington, DC, USA, contributing to several World Development Reports; Joint Research Centre (JRC) of the European Commission, Italy; and the International Rice Research Institute (IRRI), Philippines, as a Senior Scientist. He is currently a Professor in spatial agriculture and food security with the Faculty of Geo-Information Science and Earth Observation (ITC), University of Twente, Enschede, The Netherlands, where he is also the Head of the Natural Resources Department. His research interests include society's greatest challenges, such as: Where, when, and how is food produced? How much is produced, what are the risks to production, and how can these risks be mitigated? How do food and people move from A to B and what happens in the event of disruptions or changes to our food transport network infrastructure?